Silicon (2*p*) surface core-level line shape of Si(111)–B

J. E. Rowe, G. K. Wertheim, and D. M. Riffe
AT&T Bell Laboratories, Murray Hill, New Jersey 07974

(Received 13 December 1990; accepted 21 January 1991)

Several recent structural studies of the Si(111)–B ($\sqrt{3}\times\sqrt{3}$) surface have established that the boron atoms occupy substitutional sites in the second full Si layer and have Si adatoms directly above them. High-resolution (~80–100 meV) Si(2*p*) core-level photoemission was used to determine the B-induced perturbation of the surface Si atoms. The samples were prepared by surface segregation from Si(111) wafers (~1.5 at. % B) after thermally removing the thin protective oxide layer on the surface. Photoemission spectra for photon energies from 110 to 140 eV show three peaks, indicative of at least two well-separated spin-orbit doublet components. Attempts to fit the data with only two components were unsatisfactory unless a Doniach–Šunjić line shape was used for the B-induced component. This suggests that the surface region influenced by the B impurities is metallic, i.e., the Fermi level lies within the B-modified valence band. The intensity of the bulk component goes through a minimum at a photon energy of 130 eV corresponding to a kinetic energy of 26 eV and is 0.19 of the total intensity. This leads to an escape depth of ~3 Å if the B-influenced region includes three layers below the adatom layer. Improved fits were obtained by using three distinct surface components. These are identified with the Si adatoms, the three B-influenced surface layers, and the Si in the third layer which directly bonded to B.

I. INTRODUCTION

Although all group-III elements (B, Al, Ga, and In) induce a $(\sqrt{3}\times\sqrt{3})R\,30°$ reconstruction when adsorbed on Si(111),[1–9] it has recently been discovered that the B-stabilized structure is unique. While the other adatoms occupy the T_4 site above a second layer Si atom, there is good evidence that B occupies a subsurface, substitutional site in the second Si layer with a Si adatom directly above it.[2,6] The observation that the $(\sqrt{3}\times\sqrt{3})R\,30°$ low-energy electron diffraction (LEED) pattern is preserved after a room-temperature deposition of 1 Å of Si strongly supports the assignment of a subsurface site for the B.[2] More direct structural methods such as x-ray and electron diffraction are consistent only with B atoms incorporated below the Si surface and adatoms of Si not B. This is not the case for the other group-III adsorbates which occupy the adatom site.[1,7–9]

This B-stabilized, reconstructed surface is an interesting candidate for spectroscopic studies of valence and core levels, and several such studies have recently appeared.[10–13] We report Si(2*p*) core-level photoemission spectra, measured as a function of electron kinetic energy, which allow a determination of the surface and bulk components, the escape depth (and its energy dependence), and also band-bending effects due to Fermi-level pinning at the surface. The relative intensities of the surface and bulk components for our samples imply that the range of influence of the substitutional B atoms extends beyond the nearest-neighbor coordination shell of the B to include all of the Si atoms in both the first- and second-neighbor shells which (for this structure) is equivalent to the outer 3 monolayers (ML). This range effect may be a more general phenomenon than has been previously supposed and should be further investigated for other Si-adsorbate systems.

Another interesting aspect of this structure is that it provides the possibility of creating an atomically sharp doping layer inside bulk Si (δ doping).[13] We have performed some preliminary experiments which show a Fermi-level shift of ~0.4 eV by growing ~2 Å of *a*-Si on top of the B $(\sqrt{3}\times\sqrt{3})R\,30°$ structure. These measurements show that the Fermi-level pinning position depends on the surface composition and suggests that the earlier photoemission measurements[13] on less heavily doped samples had less than $\frac{1}{3}$ ML of boron since their Fermi-level position also shifted toward that of the Si covered surface.

II. SAMPLE CHARACTERIZATION AND EXPERIMENTAL DETAILS

The B-doped samples used in this study were prepared from Si(111) wafers implanted with 30-keV B^{10} ions to 2×10^{16} cm^{-2}, resulting in a heavily doped layer near the surface with B concentration of $\sim1.5\times10^{20}$ cm^{-3}.[2] These wafers were then annealed at 1050 °C for 90 min, cleaned chemically, and protected by a chemically grown thin oxide layer. They were then transferred into the ultrahigh-vacuum (UHV) photoemission system at the National Synchrotron Light Source (NSLS). The boron $(\sqrt{3}\times\sqrt{3})R\,30°$ surface reconstruction was formed in UHV by heating the Si sample to 900 °C, which desorbed the protective oxide layer and allowed diffusion to form the $\frac{1}{3}$ ML B-reconstructed surface.

We have used low-energy electron diffraction (LEED), Auger electron spectroscopy (AES), electron energy-loss spectroscopy (EELS), and synchrotron radiation photoemission to characterize the resulting $\frac{1}{3}$ ML Si(111)–B $(\sqrt{3}\times\sqrt{3})$ surface.[10,11] These measurements indicate that this method of sample preparation results in a highly reproducible, extremely well ordered, and stable surface, which is somewhat less reactive than other typical Si surfaces, e.g., that of Si(100)2×1. The resulting surface showed no measurable changes of contamination as measured by LEED,

 0734-2101/91/031020-06$01.00

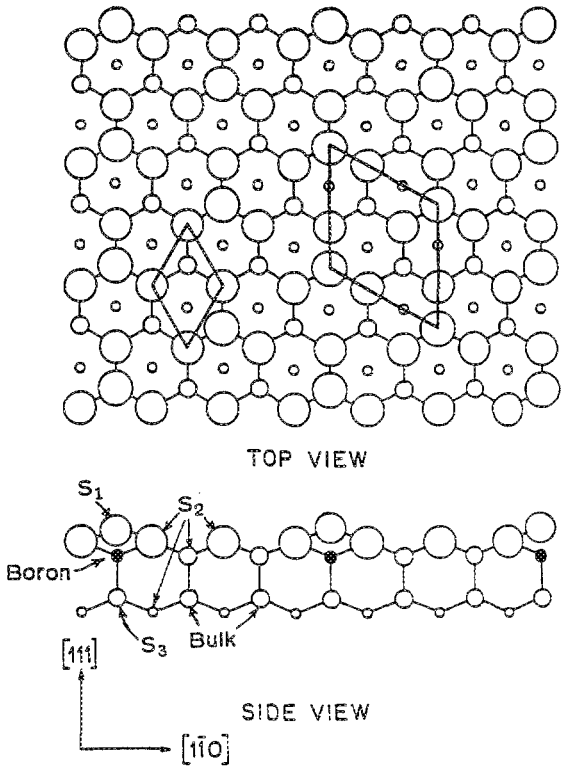

FIG. 1. Structural model for the boron ($\sqrt{3}\times\sqrt{3}$) surface showing both top view (upper panel) and side view (lower panel). The boron atoms are indicated by solid circles and the silicon atoms are indicated by open circles. The Si adatoms are located directly above the boron subsurface sites and are indicated by larger open circles.

AES, EELS, and photoemission for several hours after preparation. Moreover, unlike earlier workers,[13] we found no changes in the Si(2p) core-level photoemission spectra with repeated annealing cycles. We attribute this difference to the higher concentration of B in the bulk of our samples which diffused to the surface more readily than in less heavily doped samples used in the other study.

Recent structural studies show the $\frac{1}{3}$ ML B–Si(111) ($\sqrt{3}\times\sqrt{3}$)R 30° surface has B atoms in a second-layer substitutional site, with $\frac{1}{3}$ ML of Si adatoms directly above them constituting a fifth neighbor in the near-neighbor coordination shell,[2–5] as illustrated in Fig. 1. The upper panel shows a top view with the 1×1 and ($\sqrt{3}\times\sqrt{3}$) unit meshes both shown, and the first-layer Si and the Si adatoms are drawn as large open circles with deeper layers of Si shown as smaller open circles. The side view in the lower panel shows the B atoms in a second layer substitutional site as filled circles. They are hidden below the Si adatoms in the top view. Also labeled in the side view are the regions S_1, S_2, and S_3 corresponding to the surface core-level components found in the best-fit photoemission analysis. The bulk contribution to the core-level spectrum is due to atoms in the third layer and in the fifth and deeper layers.

Core-level photoemission experiments were performed using a high-resolution 100-mm VSW hemispherical electron spectrometer coupled to the AT&T Bell Labs–Oregon 6-m toroidal grating monochromator beamline (U4A) at the NSLS. The experimental energy resolution was 40 meV and the measured photon resolution was 70–90 meV.[14] All photoemission measurements were done at room temperature.

The surface states and valence bands of our heavily doped samples were also studied using angle-resolved photoemission spectroscopy on beamline U4A.[11] These experiments as well as the core-level photoemission data confirm recent studies showing that the B-reconstructed region is ~3 Å thick or about three atomic layers. Our measurements show a weak metallic Fermi edge that indicates that this surface region has metallic conductivity with a Fermi-level close to the maximum of the bulk valence band. Thus there is no space-charge depletion as there is on Si(111)7×7 (Refs. 15 and 16) and Si(100)2×1 surfaces. Moreover, we have observed free-carrier plasmon excitations characteristic of the bulk B doping density, near the surface extending 100–1000 Å into the bulk.[10] The $\frac{1}{3}$ ML concentration of boron was verified experimentally using secondary-ion mass spectrometry (SIMS),[15,18] but the effective thickness could not be accurately determined by SIMS due to its limited depth resolution.

III. CORE-LEVEL PHOTOEMISSION SPECTRA

The Si(111)–B($\sqrt{3}\times\sqrt{3}$)R 30° surface structure gives rise to the deceptively simple looking Si(2p) core-level photoemission spectra shown in Fig. 2, which indicate that the near-surface region sampled by photoemission is highly ordered. (The solid lines through the data points are the result of least-squares analyses described in the following section.) The Si(2p) spectra consist of three well-resolved peaks, indicative of two overlapping spin-orbit split doublets, as reported in the previous study.[13] In this interpretation, the doublet at lower binding energy is due to the bulk Si and the other one due to the B-shifted surface layer. This is reasonable from a chemical viewpoint because B is more electronegative than Si, and thus withdraws electrons from neighboring Si atoms, increasing their core-level binding energy.

The identification of bulk and surface features is confirmed by the kinetic energy dependence of the intensity of the components of the Si(2p) core-level spectra. The spectra presented in Fig. 2 were obtained with photon energies of 110, 120, 130, and 140 eV. Since the binding energy of the bulk Si($2p_{3/2}$) component is 99.30 eV and the sample work function is 4.9 eV, the electron kinetic energy varies from 6.8 to 36.8 eV for the photon energies employed. As is well known, the electron mean free path (escape depth) varies rapidly with kinetic energy in this range, and has a minimum near 25 eV for silicon.[13] The surface signal does indeed reach its maximum relative intensity near this energy.

It is clear that our data show a much stronger surface component than those reported in the previous work.[13] This is due to the (nearly) complete occupancy of the $\frac{1}{3}$ ML B sites in our samples. The fact that our spectra, unlike those in Ref. 13, did not depend on annealing procedures offers proof that the surface was totally B saturated. For a typical escape depth of ~3 Å the large intensity of the B-affected surface signal must contain contributions from more than the near-

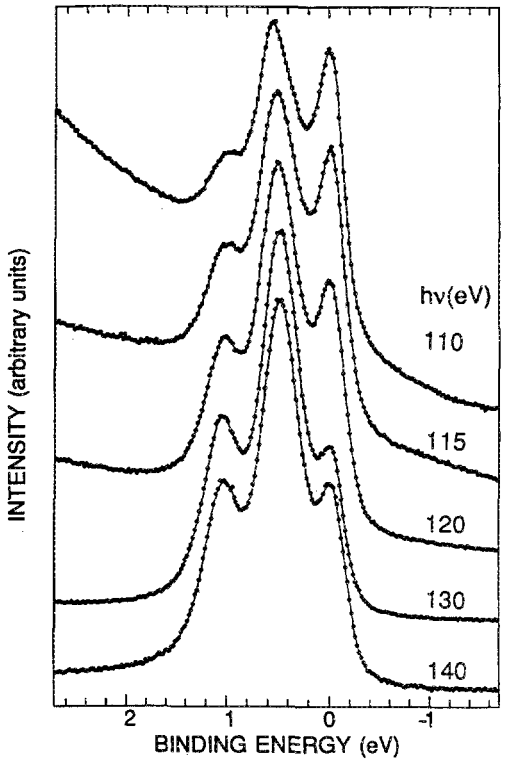

FIG. 2. Photoemission spectra of the Si(2p) core-level region for $\frac{1}{3}$ ML B/Si(111) for photon energies from 110 to 140 eV. The solid lines are the result of a least-squares fit (see text). The bulk Si($2p_{3/2}$) binding energy is 99.30 eV measured with respect to the Fermi energy. The B-influenced surface region is ~3 Å thick.

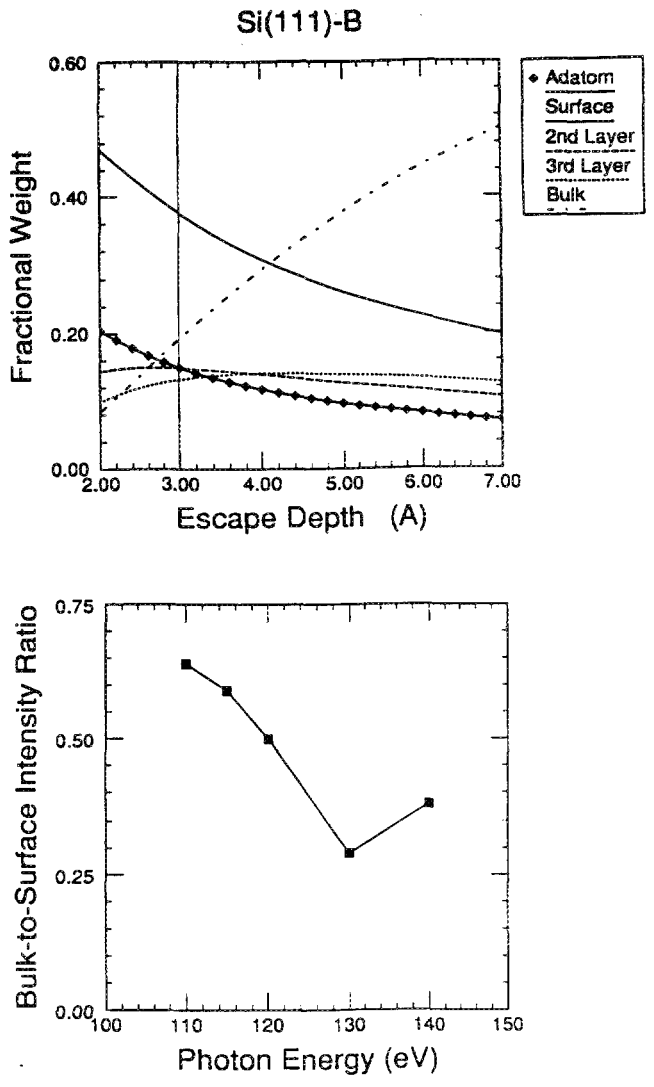

FIG. 3. Calculated fractional weights vs escape depth of the structural model shown in Fig. 1 (upper panel) and measured bulk-to-surface intensity ratio vs photon energy. For the calculated weights an equal attenuation per atomic layer was assumed so that the Si-adatom layer had weight of $\frac{1}{3}$ monolayer. The surface and bulk intensities in the lower panel were obtained from a two-component fit to the data in Fig. 2.

est-neighbor shell of Si atoms around the B site. For the structure shown in Fig. 1, we have calculated the layer-dependent fractional weight versus escape depth, assuming an exponential attenuated by the overlying atoms. The results of these calculations are plotted in the top panel of Fig. 3, with the typical escape depth of 3 Å marked by a vertical line. In order to account for the non-jellium-like charge density of bulk Si, we have treated each of the (111) double planes for the diamond lattice as having equal attenuation. Since the total distance of the (111) double layer should be preserved, this procedure leads to an average (111) layer spacing of 1.565 Å. The weight of each layer is then given by $n_i \exp(-z_i/\lambda)$, with n_i the number of atoms in the ith layer and z_i the distance of the ith layer from the adatom layer (in angstroms). At this escape depth the bulk signal, from the fourth and deeper layers, contributes only 19% of the total Si(2p) intensity. The adatom signal is even less, 15% of the total.

Still relying on the two-component model we can determine the bulk-to-surface intensity ratio for the data shown in Fig. 2. These results, shown in the lower panel of Fig. 3, are somewhat different from those obtained in the previous core-level photoemission study.[13] Not shown are measurements of the calibrated Fermi-level position versus photon energy because for our heavily B doped samples, we found this position to be constant to within ± 30 meV. These differences in surface-to-bulk intensity ratio and Fermi-level position from those of the previous study[13] are due to the improved sample preparation employed here. It is clear from the present results that the B-shifted Si(2p) surface signal originates from a much larger number of atoms than the nearest-neighbor shell, which contains only $\frac{4}{3}$ ML. For the clean Si(100)-(2×1) surface at $h\nu = 130$ eV, the $\frac{1}{3}$ ML surface signal has only ~$\frac{1}{3}$ of the bulk intensity, while in a simple two-component fit the surface signal of the Si(111)–B surface is ~3 times that of the bulk.

IV. PHOTOEMISSION LINE SHAPE ANALYSIS

Close inspection of the raw data in Fig. 2 shows a photon-energy-dependent width of the large B-shifted peaks, suggesting that a more detailed model of the data is appropriate than the two-component fit considered above. Spin-orbit

stripping to isolate the $2p_{3/2}$ contribution reveals the two components discussed in the previous section, a narrow one representing the bulk and a broader one representing the B-influenced surface region. Since the width of the B-shifted surface peak (as well as its intensity) was found to be dependent on photon energy, we used a model function for the data with additional components. However, attempts to fit the data with up to five symmetrical Voigt lines were unsatisfactory, in that many weak components with decreasing intensity are needed at ever larger binding energies to obtain a satisfactory fit. Much better but still not entirely satisfactory results were obtained when the B-influenced component was given the asymmetrical Doniach–Šunjić line shape, appropriate for core-level photoemission spectra in metals. This suggests that the B-influenced layer is metallic, i.e., the Fermi level lies within the B-modified valence band. For these least-squares fits, the singularity index was small, typically 0.06, as one might expect for a relatively small density of states near the Fermi level. The density of states at the Fermi level in our samples is known to be small, perhaps 10 times higher than that of graphite at room temperature.

The fractional intensity associated with the B-influenced Si($2p$) component is so large, that Si atoms in the first three layers must be affected by the B. This region includes at least five Si atoms with different near-neighbor environments (see Fig. 1), indicating that the larger width of the B-influenced layer is due at least in part to inhomogeneous broadening.

Although the contributions from these inequivalent atoms are not resolved, the quality of the least-squares fit is significantly improved when additional components are included in the model. Our "best" fit, shown in Fig. 4, has three surface components in addition to the bulk component. They are labeled S_1, S_2, and S_3 in order of increasing depth below the surface, relating them to the correspondingly labeled atoms in Fig. 1. The component S_1 is due to the $\frac{1}{3}$ ML of Si adatoms located directly above the subsurface B site. The component S_2 includes the monolayer of Si atoms in the first layer, which are all directly bonded to B, as well as the second neighbors in deeper layers. The second layer contributes only $\frac{2}{3}$ ML because B atoms occupy the remaining $\frac{1}{3}$ ML. The final contribution to S_2 probably comes from the 1 ML of second neighbors in the fourth layer, making for a total of $\frac{8}{3}$ ML. The $\frac{1}{3}$ ML of Si atoms in the third layer directly below the B site produce the weak S_3 component which is shifted by local strain effects. The other $\frac{2}{3}$ ML in the third layer contribute to the bulk signal along with the fifth and deeper layers.

The largest surface component, S_2, has a Doniach–Šunjić line shape while the other components have Voigt function shapes. (The fit is not sensitive to the line shape of the weaker components.) Support for the use of this metallic line shape comes from angle-resolved photoemission measurements of the valence-band features. Typical data, for photon energies of 17, 19, and 21 eV and normal emission, are shown in Fig. 5. A broadened metallic Fermi function edge, similar to that of a metal at the same experimental resolution, is found. A more complete discussion of these valence-band results will be presented elsewhere.[10]

The residuals of least-squares fits with (a) a single surface component, (b) two surface components, and (c) three sur-

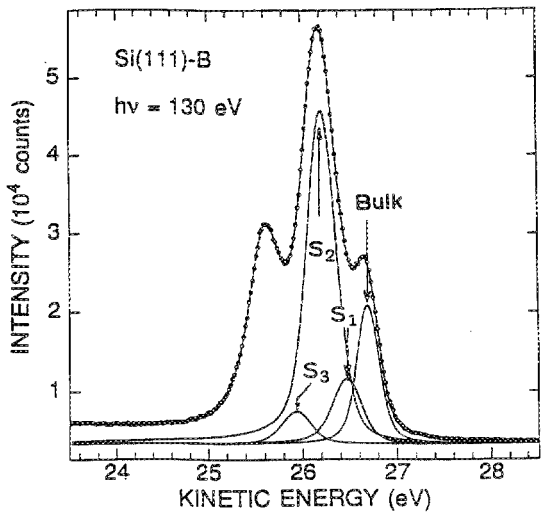

FIG. 4. Photoemission data and fitted Si($p_{3/2}$) components for photon energy, 130 eV. The bulk component and surface components, S_1 and S_3, were assumed to have a symmetric Voigt function line shape, while the B-shifted component, S_2, required an asymmetric Doniach–Šunjić line shape with $\alpha = 0.06$.

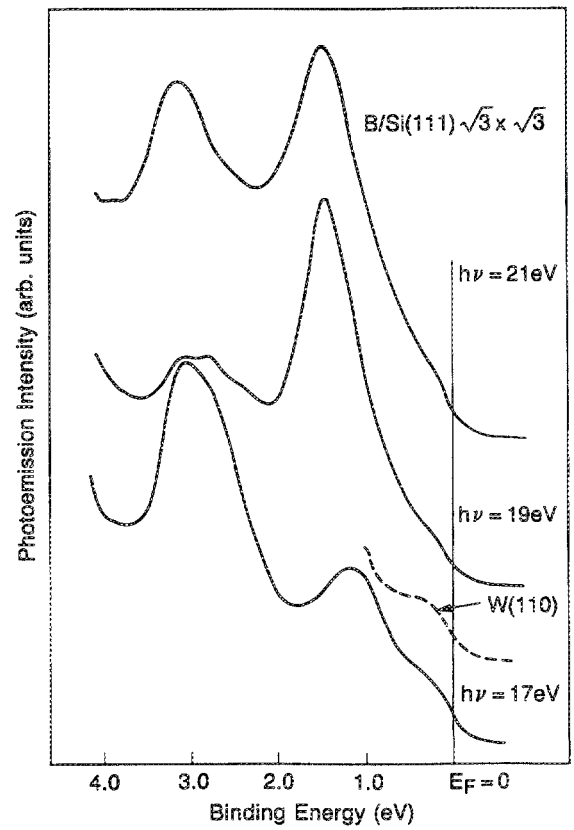

FIG. 5. Ultraviolet photoemission spectra for a normal emission collection geometry showing two prominent B-induced valence-band surface-state features and a broad shoulder near $E = 0$ eV. This weak Fermi edge indicates that the boron surface region is "metallic" and thus the screening of the Si($2p$) core hole for the B-influenced Si may be like that of a metal.

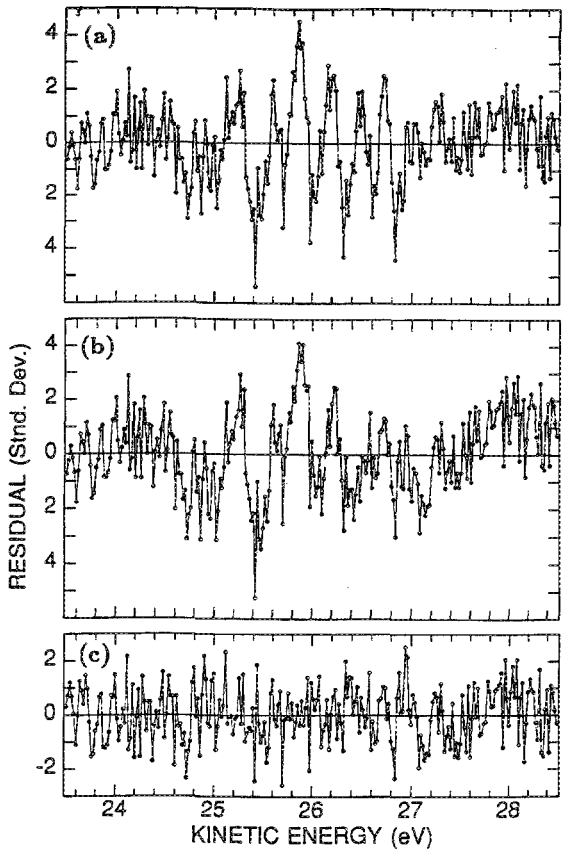

FIG. 6. Least-squares-fit residuals for (a) two components, (b) three components, and (c) four components of the Si(2p) core-level model used to interpret the photoemission data. The residuals are expressed in units of standard deviations from the fitted value at each point.

face components are shown in Fig. 6. The three fits themselves look very similar to the one shown in Fig. 4, because the deviations from experimental data points vary by only a few times the statistical noise. However, we take the absence of systematic structure in the residuals as the criterion which identifies a physically meaningful result.[19] Thus, we do not find the two- or three-component fits acceptable since both have structure in the residuals near the points of maximum slope in the raw data. Only in the fit with four components (three surface components) do we obtain *random* residuals, that fall within ± 2 standard deviations of the fitted curve. Of the three fits described above, this one should provide the most reliable and physically meaningful information. Additional components did not result in a significant improvement in the residuals, and were strongly correlated with the four components of the best fit, i.e., the additional components were not statistically independent.

Least-squares fits with completely unconstrained parameters yield values for the spin-orbit splitting of 606 ± 3 meV, in good agreement with the reported values. The spin-orbit ratios were close to the statistical value of $\frac{1}{2}$. The Lorentzian natural lifetime width of the Si(2p) lines was found to be 115 ± 10 meV. This is significantly larger than the bulk value of 80 meV obtained by XPS, and may indicate that some inhomogeneous broadening affects the determination of this parameter. It is, however, significantly smaller than values reported in the analysis of other Si surfaces, which are typically 160 meV. The Gaussian width of the bulk line is 225 meV FWHM. After correction for the instrumental resolution this becomes 206 meV, again somewhat larger than the XPS value of 140 meV, but smaller than values obtained in other surface studies. This width is presumably due to phonon. The Gaussian width of the surface component is significantly larger, 275 meV. This increase should probably not be attributed solely to phonon effects, because there is undoubtedly some inhomogeneous broadening. Additional temperature dependent photoemission measurements are required in order to separate the phonon broadening from other broadening effects.

V. DISCUSSION AND CONCLUSIONS

We have studied the core-level photoemission line shape of the $(\sqrt{3}\times\sqrt{3})$ Si(111)–B surface, prepared by surface segregation of B from the bulk. The best least-squares fit contains three surface components (S_1, S_2 and S_3) which we assign to the following structural regions: (1) a Si adatom layer ($\frac{1}{3}$ ML), (2) a B-influenced region of first- and second-neighbor Si atoms ($\frac{8}{3}$ ML), and (3) a third layer Si ($\frac{1}{3}$ ML) shifted additionally by local strain effects. The B-shifted signal, S_2, has a metallic Doniach–Šunjić line shape, which is consistent with valence-band photoemission showing a weak Fermi edge. These surface components vary in intensity relative to the bulk component with electron kinetic energy as expected for the known escape depth dependence on energy.

The intensity of the bulk component passes through a minimum for a photon energy of 130 eV, i.e., at a kinetic energy of ~ 26 eV. In this spectrum the fractional intensity associated with the bulklike Si is 0.19. This is in accord with an escape depth of 3.0 Å if the B-influenced region (lines S_1, S_2, and S_3) comprises the three outermost layers as well as the adatom. This interpretation leads to the assignment of the weak component that lies between the two strong lines to the adatom. There are two reasons for this identification. First, by analogy with the interpretation of the spectra of other Si surfaces, one would expect the adatom to have a smaller binding energy than the other surface atoms. Second, in the three-surface-component fit the fractional intensity of S_1 is 0.12, while the expected one is 0.15. The small discrepancy may not be significant, since the intensities of the two weak contributions to the complete spectrum are not well determined, but it suggests that the surface may not be fully passivated by adatoms.[3,4] The identification of the other weak component with the atom in the third layer, which is directly bonded to the B atom, is more speculative. However, even this weak component has the expected intensity for $\frac{1}{3}$ ML attenuated by the layers above (see Fig. 1). In addition, LEED intensity analysis finds a much shorter bond (2.18 Å) for these atoms compared to others in the same layer (2.39 Å) so that the chemical state might well be different.[5]

In summary, we have made a detailed interpretation of the Si(2p) photoemission line shape and found three surface components and a bulk component. The strongest surface component includes interactions with both first- and sec-

ond-neighbor Si sites (§ ML) and is characterized by a metallic Doniach–Šunjić line shape due to the finite density of states at the Fermi level. This second-neighbor contribution is contrary to most other core-level shifts where only first-neighbor interactions have been identified, but there is some evidence that (at least for Si) longer-range interactions are important.[20] It is possible that the metallic nature of the valence electrons of this surface is correlated with this second-neighbor shift effect. It would be desirable to perform high-resolution photoemission experiments on other "dopant" atoms such as Al, Ga, In, As, and Sb in order to investigate this possibility.

ACKNOWLEDGMENTS

We are pleased to acknowledge the invaluable technical assistance of D. N. E. Buchanan, E. E. Chaban, and R. A. Malic during the course of these experiments. A special acknowledgement goes to Randy Headrick who devised the sample preparation scheme which gave such highly reproducible surfaces. Photoemission research was carried out at the National Synchrotron Light Source (NSLS), Brookhaven National Laboratory, which is supported by the Department of Energy, Division of Materials Sciences, and Division of Chemical Sciences.

[1] J. M. Nicholls, B. Reihl, and J. E. Northrup, Phys. Rev. B **35**, 4137 (1987).
[2] R. L. Headrick, I. K. Robinson, E. Vlieg, and L. C. Feldman, Phys. Rev. Lett. **63**, 1253 (1989).
[3] P. Bedrossian, R. D. Meade, K. Mortensen, D. M. Chen, J. A. Golovchenko, and D. Vanderbilt, Phys. Rev. Lett. **63**, 1257 (1989).
[4] I. W. Lyo, E. Kaxiras, and Ph. Avouris, Phys. Rev. Lett. **63**, 1261 (1989).
[5] H. Huang, S. Y. Tong, J. Quinn, and F. Jona, Phys. Rev. B **41**, 3276 (1990).
[6] H. Hirayama, T. Tatsumi, and N. Aizaki, Surf. Sci. **193**, L47 (1988).
[7] V. V. Korobotsov, V. G. Lifshits, and A. V. Zotov, Surf. Sci. **195**, 466 (1988).
[8] F. Thibaudau, P. Dumas, P. Mathiez, A. Humbert, D. Satti, and F. Salvan, Surf. Sci. **211/212**, 148 (1989).
[9] S. Benaleh, J. P. Lacharme, and C. A. Sebenne, Surf. Sci. **211/212**, 586 (1989).
[10] J. E. Rowe, R. A. Malic, E. E. Chaban, R. L. Headrick, and L. C. Feldman, J. Electron Spectrosc. Relat. Phenom. (to be published).
[11] J. E. Rowe, R. L. Headrich, and L. C. Feldman, J. Vac. Sci. Technol. (to be published).
[12] E. Kaxiras, K. C. Pandey, F. J. Himpsel, and R. M. Tromp, Phys. Rev. B **41**, 1262 (1990).
[13] A. B. McLean, L. J. Terminello, and F. J. Himpsel, Phys. Rev. B **41**, 7694 (1990).
[14] G. K. Wertheim, J. E. Rowe, D. M. Riffe, and N. V. Smith, *Proceedings of the X-90 Conference on X-ray Spectroscopy and Inner Shell Ionization Phenomena* (American Institute of Physics, New York, 1990).
[15] R. L. Headrick, A. F. J. Levi, H. S. Luftman, J. Kovalchick, and L. C. Feldman, Phys. Rev. B (in press).
[16] B. N. J. Persson and J. E. Demuth, Phys. Rev. B **30**, 5968 (1984).
[17] L. H. Dubois, B. R. Zegarski, and B. N. J. Persson, Phys. Rev. B **35**, 9128 (1987).
[18] R. L. Headrick (private communication).
[19] G. K. Wertheim and S. B. DiCenzo, J. Electron Spectrosc. Relat. Phenom. **37**, 57 (1985); **40**, 301 (1986).
[20] R. D. Bringans, M. A. Olmstead, R. I. G. Uhrberg, and R. Z. Bachrach, Phys. Rev. B **36**, 9569 (1987).